Hindawi
Wireless Communications and Mobile Computing
Volume 2021, Article ID 7400156, 15 pages
https://doi.org/10.1155/2021/7400156

Research Article

A Joint Channel Allocation and Power Control Scheme for D2D Communication in UAV-Based Networks

Enchang Sun,[1] **Hanxing Qu**,[1] **Yongyi Yuan**,[1] **Meng Li**,[1] **Zhuwei Wang**,[1] **and Dawei Chen**[2]

[1]*The Faculty of Information Technology, Beijing University of Technology, Beijing 100124, China*
[2]*Department of Electrical and Computer Engineering, University of Houston, Houston, TX, USA*

Correspondence should be addressed to Enchang Sun; ecsun@bjut.edu.cn

Received 8 July 2021; Accepted 22 September 2021; Published 26 October 2021

Academic Editor: Stefan Panic

With the increasing application of unmanned aerial vehicles (UAVs), UAV-based base stations (BSs) have been widely used. In some situations when there is no ground BSs, such as mountainous areas and isolated islands, or BSs being out of service, like disaster areas, UAV-based networks may be rapidly deployed. In this paper, we propose a framework for UAV deployment, power control, and channel allocation for device-to-device (D2D) users, which is used for the underlying D2D communication in UAV-based networks. Firstly, the number and location of UAVs are iteratively optimized by the particle swarm optimization- (PSO-) Kmeans algorithm. After UAV deployment, this study maximizes the energy efficiency (EE) of D2D pairs while ensuring the quality of service (QoS). To solve this optimization problem, the adaptive mutation salp swarm algorithm (AMSSA) is proposed, which adopts the population variation strategy, the dynamic leader-follower numbers, and position update, as well as *Q*-learning strategy. Finally, simulation results show that the PSO-Kmeans algorithm can achieve better communication quality of cellular users (CUEs) with fewer UAVs compared with the PSO algorithm. The AMSSA has excellent global searching ability and local mining ability, which is not only superior to other benchmark schemes but also closer to the optimal performance of D2D pairs in terms of EE.

1. Introduction

Integrating unmanned aerial vehicles (UAVs) into the fifth generation (5G) and beyond cellular networks is a promising technology. UAVs can be used as aerial communication platforms to assist ground communications, such as traffic offloading, recovery after natural disasters, emergency response, and Internet of Things (IoT) [1]. To solve the problem of wireless connectivity for devices that are without infrastructure coverage, such as mountainous areas and isolated islands, especially interruption of communications caused by disasters, many efforts have been made to study wireless communication with UAVs [2–8]. Compared with terrestrial communications, UAVs are generally easier to deploy, more flexible to reconfigure, and better in communication channel performance [2]. Meanwhile, [3] studies the measurement and models of air access channels between UAVs and base stations (BSs) in typical urban and rural macrocell scenarios, which is helpful to develop more reliable and more efficient communication technologies for UAVs to access the territorial cellular networks. On the other hand, the authors of [4] focus on maximizing the coverage of UAV-based BSs under the constraint of the transmitting power. In [5], a unified framework for a UAV-assisted emergency network in disasters is established. Furthermore, there is also literature combining UAVs with full-duplex mode, 6G, and other technologies. A method of uplink and downlink transmission resource allocation for a UAV-assisted full-duplex nonorthogonal multiple access system is proposed in [6], which guarantees the QoS of users and minimizes power consumption. In [7], the problem of multisource destination pair relay of UAV based on full-duplex is studied. In the aspect of user scheduling based on time division multiple access (TDMA), UAV dynamic trajectory, and UAV transmission power, the authors propose and solve a joint optimization problem to maximize the

swallowing performance of the network. However, this paper does not study the mobility of ground users. In [8], using low-altitude platforms (LAPs) and high-altitude stations, the authors propose a 6G heterogeneous Internet of Things based on XAPS and a multi-UAV cluster nonorthogonal multiple access systems. By optimizing spectrum allocation, power control, horizontal coordinates, and hovering height of UAV, the uplink accessibility and speed of the whole system can be maximized. However, existing literature has rarely investigated the UAV deployment problem and the power control and channel allocation of D2D pairs in a D2D-abled UAV-based system. The purpose of this paper is to study a scenario lacking ground BSs (GBS), such as mountainous areas, isolated islands, and disaster areas. Several UAVs that served as aerial BSs can provide communication links for areas lacking infrastructures with the help of D2D communications. However, in these emergencies, reasonable UAV deployment can reduce the interference and improve the communication quality of users; energy-efficient schemes are also required along with improving the quality of communication services.

At present, according to different optimization objectives, many scholars have proposed a variety of deployment methods of UAVs, such as minimizing the number of UAVs, minimizing deployment delay, and maximizing coverage range. To reduce the deployment delay and improve efficiency of UAVs, [9] proposes a rapid UAV deployment scheme based on bandwidth resources. By using the improved Kmeans algorithm, the goal of minimizing the number of UAVs and deployment delay is achieved, and the satisfaction of users is improved. However, the heights of UAVs are just estimated in [9]. In [10], the authors not only consider the optimization of horizontal positions but also optimize the height deployment of UAVs and propose a 3D (three-dimensional) deployment method of UAVs based on particle swarm optimization. In [11], three basic deployment designs of UAVs, namely, the minimum number of UAVs, the optimal deployment location, and the optimal transmission power allocation, are studied in combination with the instantaneous signal to the signal-to-interference-plus-noise ratio (SINR) transmitting power allocation, and the particle swarm optimization- (PSO-) based scheme is proposed. Aiming at the optimization of task completion time and overall energy consumption of multiple UAVs in resource-constrained unsaturated postdisaster areas, [12] studies the problem of data dissemination of multiple UAVs. However, the above literatures do not consider the situation that the locations of users are unknown. The related algorithms based on machine learning methods solve this problem well. The authors of [13] propose a 3D deployment method and 3D dynamic motion acquisition method of UAVs based on Q-learning. As an agent, each UAV makes its own 3D positioning decision through trial and error learning. In [14], a geographic location information learning algorithm is proposed, which avoids accurate channel calculation, saves a lot of time, fills the blank of quickly establishing multiple UAVs to serve multiple users, solves the problem of how to find suitable base station location for multiple UAVs as soon as possible, and achieves the goal of maximizing the total downlink rate of the communication network. [15] utilizes game theory and machine learning methods to deploy the 3D position of UAV to compensate for interruption and overload of the network. This method does not need to know all the information of the system and a large amount of network information exchange. In order to learn and adapt to time-varying user activities, the authors of [16] study the deployment of dynamic UAVs. Without knowing the users' time activity distribution parameters, UAV can update the belief about the activity probability of undiscovered users according to the visit history. Finally, the Q-learning algorithm is applied to develop effective deployment strategies.

Many scholars have studied UAV-aided networks. In [17], the authors propose an energy-efficient multi-UAV coverage model based on spatial adaptive strategy. In [18], the authors try to maximize the energy efficiency (EE) of UAVs by designing the trajectory path of UAVs, considering both throughput and propulsion energy consumption of UAVs. Literature [19] studies the joint optimization of the UAV track, aimed at minimizing the total energy consumption of each node under the constraint that the estimated mean square error is less than the target threshold. To solve the problem of resource allocation and trajectory design for multi-UAV-aided cellular networks with unreachable user location and channel parameters, the authors of [20] propose a multiagent reinforcement learning solution to optimize the overall throughput and fairness throughput. With the exponential growth of data traffic, the use of caching and D2D communication has been recognized as an effective approach for mitigating the backhaul bottleneck in UAV-assisted networks in [21]. The authors of [22] consider a scenario that UAV-BS replaces destroyed traditional GBSs when a natural disaster occurs; a large-scale UAV is deployed to provide wireless service to ground devices with the support of D2D-enabled links. However, one UAV can only serve a small limited range of signal coverage. Meanwhile, in [23], the optimization of power control for D2D communication underlying UAV-assisted access systems is investigated, but channel allocation is not considered. In order to improve the above deficiencies, in this paper, a D2D-abled UAV-based system with multiple UAVs is considered, and the UAV deployment and D2D energy efficiency are optimized in two steps.

To date, existing literature has investigated the UAVs' deployment and the D2D pairs' EE on an underlay D2D-enabled UAV-based network. The main contributions of this paper are as follows.

(i) We aim to minimize UAVs' number and deployment to achieve a given SINR requirement, by using the particle swarm optimization- (PSO-) Kmeans algorithm. Under the condition of not exceeding the coverage of UAVs, the less quantity and better deployment of UAVs make cellular user (CUE) less interference while better communication quality

(ii) After determining the deployment of UAVs, we improve EE of D2D pairs while considering QoS

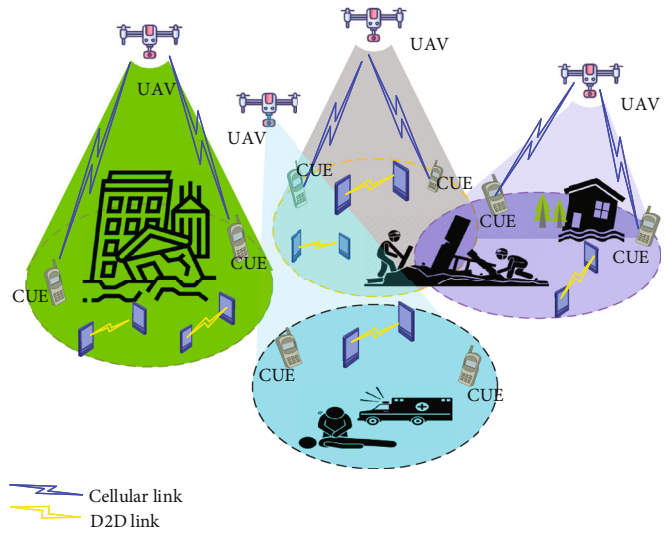

Figure 1: The system architecture.

constraints in a D2D-abled UAV-based system, which is a complicated NP-hard problem

(iii) By introducing the population variation strategy and the leader-follower adaptive adjustment strategy, the adaptive mutation salp swarm algorithm (AMSSA) is proposed to solve the optimization problem, such that the variation of nonoptimal individuals can improve the diversity of the population and make the iteration easier to achieve global optimization. Meanwhile, the adaptive leader-follower numbers can have a better balance between exploration and development capabilities, and the adaptive weights updating strategy makes it easier for AMSSA to jump out of the local optimum. Furthermore, the Q-learning strategy enables the salps to choose the individuals to follow, thus refusing blind following

(iv) Finally, we propose an efficient iterative resource allocation algorithm; the problem of optimizing D2D pairs' EE can be solved by the proposed AMSSA

The rest of this paper is organized as follows. In Section 2, the system modeling and the interference modeling are introduced. In Section 3, we analyse the UAV deployment problem and introduce the PSO-Kmeans algorithm. The model and proposed method of power control and channel allocation are given in Sections 4 and 5, respectively. Simulation results are shown in Section 6, and conclusions are drawn in Section 7.

2. System Modeling

In this section, the system modeling and the interference modeling of CUEs and D2D pairs are illustrated in Subsections 2.1–2.3, respectively.

2.1. System Modeling. The system model is shown in Figure 1. In some remote areas and extreme cases, such as mountainous areas and isolated islands where there is no GBS, as well as disaster areas where GBSs are out of service, the rapid provision and recovery of communication are significant for people's production, life, and disaster relief. Therefore, in this paper, several UAVs are deployed as aerial BSs to provide temporary communication connections for users, so as to solve the communication interruption caused by GBS absence. In a short time, we assume that UAVs are still in the air, which can provide stable communication for users within the coverage area. We consider reusing uplink resources because reusing downlink resources is more difficult and less effective than reusing uplink resources in a cellular network [24]. Therefore, this paper focuses on the resource allocation of uplink, and the related research of downlink will be studied in the future.

We consider an interference-limited D2D system for a single-cell uplink scenario in which the ground base station does not exist. The UAVs are temporary aerial BSs. The users are distributed randomly in cells. Assume that each UAV is stationary in a short time; in this case, each UAV-BS controls several CUEs and surrounding D2D pairs, and each CUE or D2D pair can only be controlled by one UAV-BS. The cellular transmissions under the control of a UAV-BS are orthogonal while CUEs in disparate UAV-BSs can reuse the same channels. Similarly, a D2D pair can reuse only one CUE channel of the same UAV, and one CUE channel can be reused by multiple D2D pairs. The UAV-BS contains the complete information of the instantaneous channel state information of links to all UEs, which are assumed to be independent block fading, and each receiver knows the fading characteristics of only its own communication link, whether it is CUE or D2D [22].

2.2. Interference Modeling of CUEs. In our system, the channels that CUEs covered by the same UAV are mutually orthogonal, so there is no interference between them. When

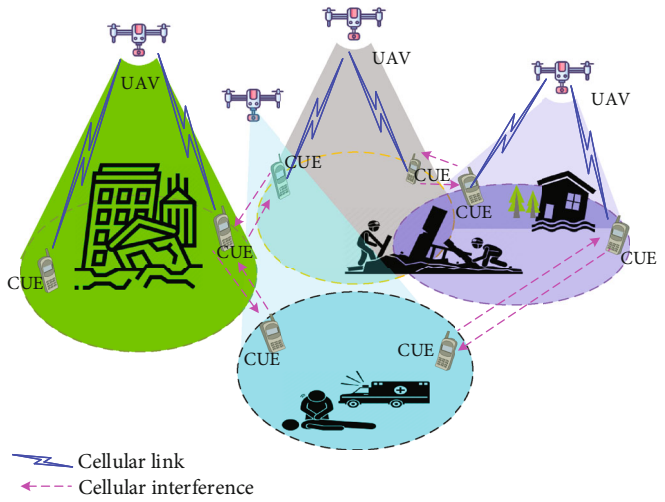

Figure 2: The interference of CUEs to UAVs.

CUEs are served by different UAVs as well as multiplex the same channel, there will be interference. Figure 2 shows the interference of CUEs to UAVs.

2.3. Interference Modeling of D2D Pairs. As described in [25], we analyse several complicated interference scenarios in the system. Figure 3 shows four different interference scenarios to D2D receivers ($D2D_R$); those are intracell interference of CUEs towards $D2D_R$, intercell interference of CUEs towards $D2D_R$, intracell interference of other D2D transmitters ($D2D_T$) towards $D2D_R$, and intercell interference of other $D2D_{Ts}$ towards $D2D_R$.

(1) *Intracell Interference of CUEs towards $D2D_R$.* As shown in Figure 3(a), in a UAV-BS, the CUE creates interference towards $D2D_R$, which reuses the same channel

(2) *Intercell Interference of CUEs towards $D2D_R$.* As shown in Figure 3(b), this kind of interference, towards $D2D_R$, is generated by CUEs in different UAV-BSs

(3) *Intracell Interference of $D2D_{Ts}$ towards $D2D_R$.* As shown in Figure 3(c), the interference is generated by other $D2D_{Ts}$, which reuse the same channel of $D2D_R$ in the same UAV-BS

(4) *Intercell Interference of $D2D_{Ts}$ towards $D2D_R$.* As shown in Figure 3(d), this scenario shows the intercell interference where $D2D_{Ts}$ comes from other UAV-BS interference with $D2D_R$

3. Minimum Number and Optimal Location Deployment Strategy of UAVs

3.1. Problem Model. In our scenario, $\forall j \in \mathcal{J} = \{1, 2, \cdots, J\}$ and $m \in \mathcal{M} = \{1, 2, \cdots, M\}$ index the jth CUE and the mth UAV, respectively. Otherwise, CUEs covered by the same UAV are orthogonal to each other, and there is no interference, but there is interference between CUEs, which are served by different UAVs while using the same channel.

We assume $C_{j,m}$ is the jth CUE that is covered by mth UAV U^m. 3D locations of $C_{j,m}$ and U^m are donated by $S_{C_{j,m}} = (X_{C_{j,m}}, Y_{C_{j,m}}, Z_{C_{j,m}})$ and $S_{U^m} = (X_{U^m}, Y_{U^m}, Z_{U^m})$, respectively. Thus, the horizontal distance between $C_{j,m}$ and U^m is defined as

$$\Delta R_j^m = \sqrt{\left(X_{C_{j,m}} - X_{U^m}\right)^2 + \left(Y_{C_{j,m}} - Y_{U^m}\right)^2}. \quad (1)$$

The vertical distance between $C_{j,m}$ and U^m is given by

$$\Delta H_j^m = Z_{U^m} - Z_{C_{j,m}}. \quad (2)$$

We consider a UAV-assisted emergency communication network. Most countries stipulate that the UAV flight height is less than 150 meters. Therefore, the path loss channel model proposed in [26] is particularly suitable for the system in this paper. LAPs are below the stratosphere, are easy to be deployed, and are consistent with the broadband cellular concept, because low altitude combines coverage advantages with limited cellular radius [26].

As described in [11, 26], the path loss channel model of LAPs can be written as

$$L_j^m = \frac{\eta_{\text{Los}} - \eta_{\text{NLos}}}{1 + qe^{-\xi\left(\varphi_j^m - q\right)}} + 10\log\left[\left(\Delta H_j^m\right)^2 + \left(\Delta R_j^m\right)^2\right] + 10\log\left(\frac{4\pi f}{v_c}\right)^2 + \eta_{\text{NLos}}, \quad (3)$$

where φ_j^m is the elevation angle between $C_{j,m}$ and U^m, which is defined as

$$\varphi_j^m = \tan^{-1}\frac{\Delta H_j^m}{\Delta R_j^m}. \quad (4)$$

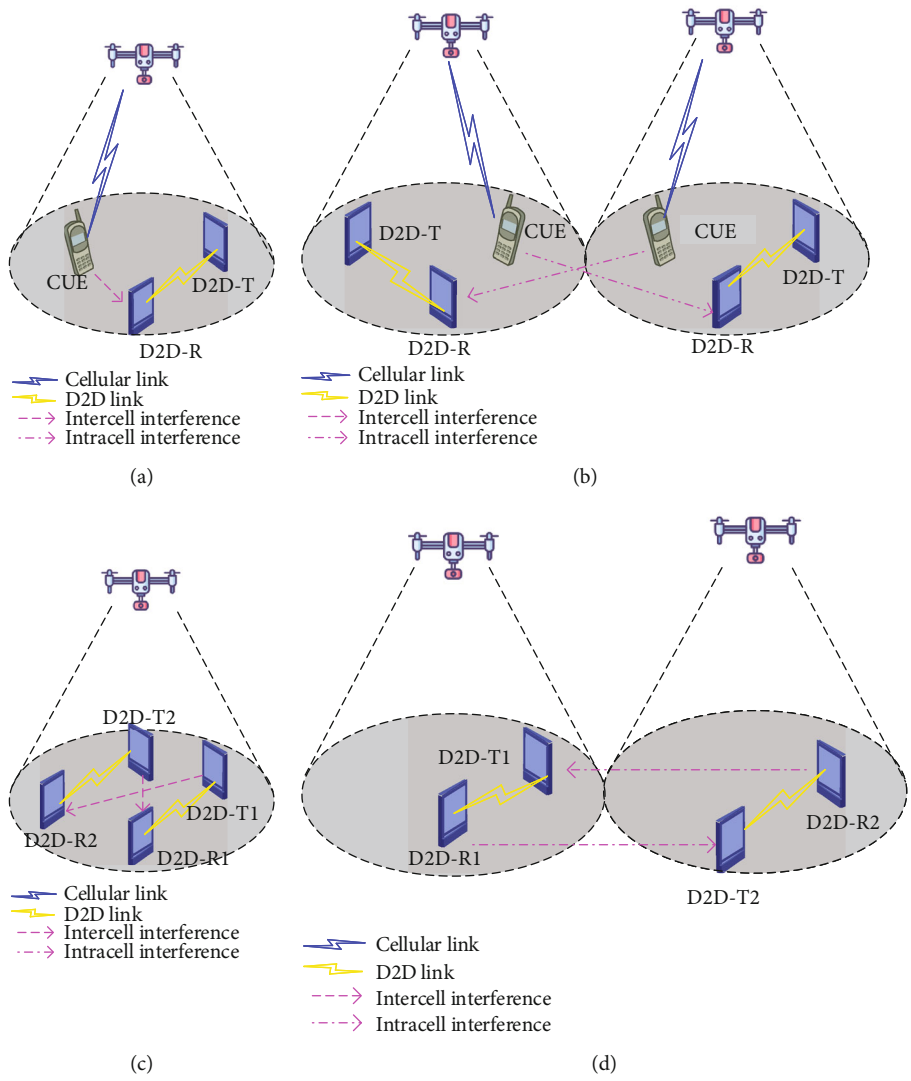

FIGURE 3: Interference scenarios to D2D receiver: (a) intracell interference of CUEs towards $D2D_R$, (b) intercell interference of CUEs towards $D2D_R$, (c) intracell interference of $D2D_{Ts}$ towards $D2D_R$, and (d) intercell interference of $D2D_{Ts}$ towards $D2D_R$.

Moreover, η_{Los}, $\eta_{N\text{Los}}$, q, and ξ are the environment parameters, f is the transmitted radio frequency, and v_c is the speed of light.

We focus on the UAV deployment optimization problem, and the small-scale fading is not considered.

Furthermore, the instantaneous signal-to-interference-plus-noise ratio (SINR) of $C_{j,m}$ can be expressed as

$$\gamma_j^m = \frac{p_{C_{j,m}} L'^m_j}{I_{j,\text{inter}} + \sigma^2}, \tag{5}$$

where

$$L'^m_j = 10^{-L_j^m/10},$$

$$I_{j,\text{inter}} = \sum_{\substack{j'=1 \\ j' \neq j}}^{J} \sum_{\substack{m'=1 \\ m' \neq m}}^{M} b_{j',j} b_{j',m'}' p_{C_{j',m'}} L'^{m'}_{j'}, \tag{6}$$

$b_{j',j}$ means the CUE association variable (i.e., if the j'th CUE and the jth CUE use the same channel, $b_{j',j} = 1$; otherwise, $b_{j',j} = 0$). $b_{j',m'}'$ means the CUE-UAV association variable (i.e., if the j'th CUE in the m'th UAV, $b_{j',m'}' = 1$; otherwise, $b_{j',m'}' = 0$). $p_{C_{j,m}}$ and $p_{C_{j',m'}}$ represent the transmit power of $C_{j,m}$ and $C_{j',m'}$, respectively. σ^2 is the aggregate power of noise.

Our UAV deployment problem is aimed at minimizing the number of UAVs and optimizing their locations. Combining (1)–(7), we can formulate the problem as follows:

$$\min M, \tag{7}$$

$$\text{s.t.} \min \gamma_e^m > \gamma_0, \tag{8a}$$

$$\left\| U^m - U^{m'} \right\|_2 > 0, \quad \forall m, m' \in \mathcal{M}, \tag{8b}$$

read M, γ_0;
Initialize positions of UAVs by using Kmeans;
while $\gamma_{\min} < \gamma_0$ **do**
$M \longleftarrow M + 1$
Initialize positions of UAVs by Kmeans;
  while $1 \le iter \le ger$ **do**
    for $1 \le par \le pop$ **do**
      $\gamma(par) \longleftarrow \sum_{m=1}^{M} \sum_{j=1}^{J} (p_{C_{j,m}} L'^{m}_{j} / I_{j,inter} + \sigma^2)$
    if $\gamma_{\text{Individual}}(par) < \gamma(par)$ **then**
      $\gamma_{\text{Individual}}(par) = \gamma(par)$
      $X_{\text{Individual}}(par) = X(par)$
    end if
  end do
    if $\gamma_{\text{Population}} < \max(\gamma_{\text{Individual}})$ **then**
      $\gamma_{\text{Population}} = \max(\gamma_{\text{Individual}})$
      $X_{\text{Population}} = \max(X_{\text{Individual}})$
    end if
  $iter \longleftarrow iter + 1$
  update v
  $X \longleftarrow X + v$
  end while
  end while
  print X;

Algorithm 1: UAV deployment scheme based on the PSO-Kmeans algorithm in D2D-abled UAV-based system.

$$\sum_{m=1}^{M} b_{j,m} \le 1, \quad \forall m \in \mathcal{M}, \tag{8c}$$

$$S_{U^m} = (X_{U^m}, Y_{U^m}, Z_{U^m}) \in \mathcal{D}, \quad \forall m \in \mathcal{M}, \tag{8d}$$

where γ_0 in (8a) is the minimum limit of the minimum SINR. Equation (8b) ensures that any two UAVs do not hover in the same position, thus effectively avoiding UAV collisions. Equation (8c) limits one CUE to only one UAV. Equation (8d) ensures that the locations of UAVs must be in the feasible area.

This UAV deployment problem is nonconvex and is hard to find the optimal solution. Thus, the PSO-Kmeans algorithm is used to solve the suboptimal solution of the optimization problem.

3.2. PSO-Kmeans Algorithm. The particle position of the PSO algorithm is random. Therefore, this paper first uses the Kmeans algorithm to generate the initial particle positions, which makes the PSO algorithm have good initial particle positions, which is beneficial to further improving the iterative performance.

Firstly, the positions of J CUEs are randomly selected as the initial positions of M clusters. We define the clusters as $\mathcal{U} = \{\mathcal{U}^1, \mathcal{U}^1, \cdots, \mathcal{U}^m\}$. The horizontal distance between C_j and the centroid of the mth cluster r^m is defined as

$$\Delta d_j^m = \sqrt{\left(X_{C_j} - X_{r^m}\right)^2 + \left(Y_{C_j} - Y_{r^m}\right)^2}. \tag{9}$$

Find the centroid which is the closest to C_j and attribute C_j to the corresponding cluster $\mathcal{U}^m$, and update $\{\mathcal{U}^m\} = \{\mathcal{U}^m\} \bigcup \{C_j\}$.

The centroid r^m is updated by

$$S_{r^m} = \frac{1}{|\mathcal{U}^m|} \sum_{C_j \in \mathcal{U}^m} S_{C_j}. \tag{10}$$

Finally, Equations (9) and (10) are repeated several times until all the centroids are no longer changed, and the initial position of the first-generation UAV is obtained, which is input into the scheme based on the PSO algorithm. The UAV deployment scheme based on the PSO-Kmeans algorithm is shown in Algorithm 1.

3.3. Complexity Analysis. At first, the initial deployment of UAVs is obtained by clustering with the Kmeans algorithm. Assuming that there are S particles in the PSO algorithm, the Kmeans algorithm needs to be repeated for S times to get S groups of UAV initial deployment as the initial position of S particles. Thus, the time complexity of S times Kmeans algorithm is $\mathcal{O}(3 \cdot J \cdot M \cdot t' \cdot S)$, where J means the number of sample points (i.e., the quantity of CUEs), M means the number of UAVs, and t' is the iterations. In addition, the time complexity of the PSO algorithm is $(J^3 \cdot t'' \cdot S)$. Thus, the time complexity of the PSO-Kmeans algorithm is $\mathcal{O}(3 \cdot J \cdot M \cdot t' \cdot S + J^3 \cdot t'' \cdot S)$.

4. Power Control and Channel Allocation of D2D Pairs

In this section, we model the energy efficiency optimization problem of D2D pairs when determining the deployment of UAVs.

Let $\forall k \in \mathcal{K} = \{1, 2, \cdots, K\}$ index the kth channel. In the mth UAV-BS, let Dr_x^m and Dt_x^m denote receiver and transmitter of the xth D2D pair D_x^m, respectively.

The intracell interference towards Dr_x^m is given by

$$I_{x,\text{intra}}^m = \sum_{\substack{i=1 \\ i \neq x}}^{X} a_{k,i} p_i^m (l_{x,i})^{-\beta} h_{x,i}^m + p_c (l_{x,c})^{-\beta} h_c^m, \tag{11}$$

where $\mathcal{X}$ means the set of X D2D pairs in the mth UAV-BS. $a_{k,i}$ is the channel state indicator variable (i.e., if D_i^m shares the same channel k with D_x^m, $a_{k,i} = 1$; otherwise, $a_{k,i} = 0$). p_i^m and p_c denote the transmit power for Dt_i^m (i.e., transmitters of other interfering D2D pairs in the same UAV-BS) and the CUE at the same channel k in the mth UAV-BS, respectively. $l_{x,i}$ and $l_{x,c}$ represent the distance between Dr_x^m and Dt_i^m, Dr_x^m and CUE, respectively. $h_{x,i}^m$ and h_c^m are the channel gains, regardless of the link being cellular or D2D, and β denotes the path loss exponent.

The intercell interference towards Dr_x^m is given by

$$I_{x,\text{inter}}^m = \sum_{\substack{m'=1 \\ m' \neq m}}^{M} \left[\sum_{i'=1}^{X'} a'_{k,i'} p_{i'}^{m'} \left(l_{x,i'}^{m'} \right)^{-\beta} h_{x,i'}^{m'} + p_{c'}^{m'} \left(l_{x,c'}^{m'} \right)^{-\beta} h_{c'}^{m'} \right], \tag{12}$$

where $\mathcal{X}'$ means the set of X' D2D pairs in the m'th UAV-BS. $a'_{k,i'}$ represents the channel state indicator variables between $D_{i'}^{m'}$ and D_x^m. It should be emphasized that $D_{i'}^{m'}$ and D_x^m are in two different UAV-BSs. $p_{i'}^{m'}$ and $p_{c'}^{m'}$ denote the transmit power of $Dt_{i'}^{m'}$ and CUE that shares the same channel k but in another UAV-BS. $l_{x,i'}^{m'}$ and $l_{x,c'}^{m'}$ are the channel gain, regardless of the link being cellular or D2D, and β denotes the path loss exponent.

Furthermore, SINR of Dr_x^m can be expressed as

$$\gamma_{Dr_x^m} = \frac{p_x^m (l_x)^{-\beta} h_x^m}{I_{x,\text{intra}}^m + I_{x,\text{inter}}^m + \sigma^2}, \tag{13}$$

where p_x^m denotes the transmit power of Dt_x^m and l_x is the propagation distance of D2D pair D_x^m. h_x^m represents the channel gain and σ^2 denoting the power spectral density of the additive white Gaussian noise (AWGN) at the receivers.

Therefore, the spectral efficiency (SE) (bit/s/Hz) of Dr_x^m is given by

$$\text{SE}_{Dr_x^m} = \log_2 \left(1 + \gamma_{Dr_x^m} \right). \tag{14}$$

The total power consumption of D_x^m, which concludes transmit and circuit power, is given by

$$p_{D_x^m} = p_{Dt_x^m} + 2p_0, \tag{15}$$

where p_0 is the circuit power of D2D pair D_x^m. The circuit power needs to be multiplied by 2, because both Dt_x^m and Dr_x^m must be taken into account.

The EE of D2D pairs (bit/J/Hz) is given by

$$\text{EE} = \sum_{m=1}^{M} \sum_{x=1}^{X} \frac{\text{SE}_{Dr_x^m}}{p_{D_x^m}}. \tag{16}$$

Our objective is to maximize the EE of all D2D pairs in the system. Combining (11)–(16), we formulate the joint power control and channel allocation problem as an optimization problem as follows:

$$\max \text{EE}, \tag{17}$$

$$\text{s.t.} \text{SE}_{Dr_x^m} > \text{SE}_{\min}, \tag{18a}$$

$$a_{k,i}, a'_{k,i'} \in \{0, 1\}, \quad \forall i, i' \in \mathcal{X}, \forall k \in \mathcal{K}, \tag{18b}$$

$$\sum_{k=1}^{K} a_{k,i} \leq 1, \sum_{k=1}^{K} a'_{k,i'} \leq 1, \quad \forall i, i' \in \mathcal{X}, \tag{18c}$$

$$0 \leq p_x^m < p_{Dt}^{\max}, \quad \forall x \in \mathcal{X}, \forall m \in \mathcal{M}, \tag{18d}$$

where $\text{SE}_{\min}$ in (18a) is the minimum SE of $D2D_R$, which satisfies the QoS requirement. Equations (18b) and (18c) mathematically model our assumption that one D2D pair can only reuse one channel. Equation (18d) ensures that the transmit powers of $D2D_{Ts}$ cannot go beyond the maximum limit.

We define A as the channel allocation matrix for all D2D pairs, in the same way, P as the power control matrix. This optimization problem is a complicated NP-hard problem, and no efficient polynomial-time solutions exist, as the complexity may increase. Therefore, we propose the quantity-weight adaptive salp swarm algorithm to solve the problem.

5. Adaptive Mutation Salp Swarm Algorithm

In this section, firstly, we introduce the salp swarm algorithm (SSA) and the adaptive salp swarm algorithm (ASSA). Then, we propose the adaptive mutation salp swarm algorithm (AMSSA), which is aimed at solving the power control and channel allocation problem.

5.1. Salp Swarm Algorithm and Adaptive Salp Swarm Algorithm. In [27], the authors propose the first model of the salp chain. The salp chain can be divided into two groups: leader salp and follower group. The leader salp is at the front of the chain, while the other salps are regarded as follower salps.

A two-dimensional matrix s is defined as the position of all salps, and an n-dimensional search space includes a food source F.

The leader salp position updates can be expressed:

$$s_w^z = \begin{cases} F_w + \alpha_1((ub_w - lb_w)\alpha_2 + lb_w), & \alpha_3 \geq 0.5, \\ F_w - \alpha_1((ub_w - lb_w)\alpha_2 + lb_w), & \alpha_3 < 0.5, \end{cases} \tag{19}$$

where $z = 1$. s_w^z is the position of the leader in the wth dimension. F_w is the food position in the wth dimension. ub_w represents the upper bound of the wth dimension, and lb_w represents the lower bound of the wth dimension. α_1, α_2, and α_3 are the constants of the interval [0, 1], respectively. Meanwhile, they dictate the next position in the wth dimension as well as the step size.

Furthermore, the update positions of follower salps are defined as

$$s_w^z = \frac{1}{2}\left(s_w^z + s_w^{z-1}\right), \tag{20}$$

where $z \geq 2$ and s_w^z shows the zth follower position in the wth dimension.

Thus, the salp chain can be simulated by (19) and (20).

It can be seen that there are two optimization matrices for the power control and channel allocation problem. Meanwhile, the channel allocation matrix A is discrete, while the power control matrix P is continuous. Thus, the continuous SSA cannot be directly used to solve the optimization problem of power control and channel allocation for maximum energy efficiency in the D2D-abled UAV-based system. The authors in [28] propose the ASSA, which can solve the above problem.

The leader salp position updates can be described as

$$A^1 = A_{\text{best}},$$
$$P^1 = \begin{cases} P_{\text{best}} + \lambda_1\lambda_2 P_d^{\max}, & \lambda_3 \geq 0.5, \\ P_{\text{best}} - \lambda_1\lambda_{2P_d^{\max}}, & \lambda_3 < 0.5, \end{cases} \tag{21}$$

where P^1 and A^1 are the leader salp position. A_{best} and P_{best} are defined as the current optimal channel allocation and power control matrix in the iterative process, respectively. λ_1, λ_2, and λ_3 are the same as α_1, α_2, and α_3 in SSA. $P_d^{\max}$ represents the maximum power constraint.

The follower salp positions are defined as

$$A^y = \begin{cases} A^y, & F(A^y, P^y) \geq F\left(A^{y-1}, P^{y-1}\right), \\ A^{y-1}, & F(A^y, P^y) < F\left(A^{y-1}, P^{y-1}\right), \end{cases}$$
$$P^y = \begin{cases} P^y + \left(\omega_{\max} - \dfrac{(\omega_{\max} - \omega_{\min})t}{T}\left(P^y - P^{y-1}\right)\right), & F(A^y, P^y) \geq F\left(A^{y-1}, P^{y-1}\right), \\ P^y - \left(\omega_{\max} - \dfrac{(\omega_{\max} - \omega_{\min})t}{T}\left(P^y - P^{y-1}\right)\right), & F(A^y, P^y) < F\left(A^{y-1}, P^{y-1}\right), \end{cases} \tag{22}$$

where A^y and P^y are follower salp positions. $\omega_{\max}$ and $\omega_{\min}$ are initial weight and final weight, respectively. $F(A^y, P^y)$ represents the fitness function, which is used to evaluate the current positions of follower salps.

However, the number of leaders and followers is fixed, which limits the searching abilities of these two algorithms. In order to overcome the above shortcomings and further improve the capability of global searching and local mining, we propose the AMSSA scheme.

5.2. Adaptive Mutation Salp Swarm Algorithm. We introduce the population variation strategy and the leader-follower adaptive adjustment strategy based on the ASSA. Firstly, the randomly generated locations of salps are mutated by the population variation strategy. Then, leader-follower adaptive adjustment strategy is used to update the position of the variation salps. Finally, the Q-learning strategy is considered to allow salps to gain autonomous following ability, which enables the individual of the salps to choose followers independently and avoid falling into local optimum due to blind following.

When the population of the salp group is fixed, there are more leaders and less followers in the initial iteration, which means AMSSA focuses on the global search. As the iteration continues, the number of leaders decreases, and the number of followers increases. In the later stage of iteration, more

read A, P

$$F_1^y \longleftarrow \sum_{m=1}^{M}\sum_{x=1}^{X}\frac{\log_2(1+\gamma_{Dr_x^m})}{p_{Dt_x^m}+2p_0}$$

while $2 \le t \le T$ **do**

update A randomly and generate P corresponding to A

$$V_{t-1}^y \longleftarrow \begin{cases} 0, F_t^y(A^y, P^y) < F_t^{y-1}(A^{y-1}, P^{y-1}) \\ 1, F_t^y(A^y, P^y) \ge F_t^{y-1}(A^{y-1}, P^{y-1}) \end{cases}$$

$$P_t^y \longleftarrow P_{t-1}^{best} + \left(1 - \sum_{y=1}^{Y}(1/Y)V_{t-1}^y\right)\left(P_t^{y'} - P_t^{y''}\right) \quad \text{f } \textbf{or } 1 \le r \le \rho N \textbf{ do}$$

$$A^{y\wedge} \longleftarrow A^{y\wedge}$$

$$P^{y\wedge} \longleftarrow \begin{cases} P_{best} + \lambda_1\lambda_2 P_d^{\max}, \lambda_3 \ge 0.5 \\ P_{best} - \lambda_1\lambda_2 P_d^{\max}, \lambda_3 < 0.5 \end{cases}$$

end do

for $\rho N \le y \le N$ **do**

$$Q^{(y,y'')} \longleftarrow r\wedge^{(y,y'')} + \epsilon \max Q^{(y)},$$

$$y'' \longleftarrow \text{argmax}\{ Q^{(y,y'')} \mid y'' \in Y\}$$

$$A^y \longleftarrow \begin{cases} A^y, F(A^y, P^y) \ge F(A^{y''}, P^{y''}) \\ A^{y'}, F(A^y, P^y) < F(A^{y''}, P^{y''}) \end{cases}$$

$$P^y \longleftarrow \begin{cases} P^y + (\mu_1 - \mu_2 t/T)(P^y - P^{y''}), F(A^y, P^y) \ge F(A^{y''}, P^{y''}) \\ P^y - (\mu_1 - \mu_2 t/T)(P^y - P^{y''}), F(A^y, P^y) < F(A^{y''}, P^{y''}) \end{cases}$$

end do

for $1 \le y \le N$ **do**

$$F_t^y \longleftarrow \sum_{m=1}^{M}\sum_{x=1}^{X}\left(\log_2(1+\gamma_{Dr_x^m})/p_{Dt_x^m}+2p_0\right)$$

if $F_t^y \ge F_{t-1}^{best}$ **then**

$$F_t^{best} \longleftarrow F_t^y$$

$$A_t^{best} \longleftarrow A_t^y$$

$$P_t^{best} \longleftarrow P_t^y$$

end if

end do

if $F_t^{best} \ge F_{t-1}^{best}$ **then**

$$F^{best} \longleftarrow F_t^{best}$$

$$A^{best} \longleftarrow A_t^{best}$$

$$P^{best} \longleftarrow P_t^{best}$$

else

$$F^{best} \longleftarrow F_t^{best}$$

$$A^{best} \longleftarrow A_t^{best}$$

$$P^{best} \longleftarrow P_t^{best}$$

end if

end do

print F^{best}, A^{best} and P^{best}

Algorithm 2: D2D energy efficiency maximization scheme based on the QWASSA in D2D-abled UAV-based system.

followers make the AMSSA focus on local search, so the AMSSA is hard to fall into local optimum.

(1) *Population Variation Strategy*. In each iteration, the randomly generated power control matrix is mutated by

$$P_t^y = P^{\text{best}} + (1 - \Gamma_{t-1})\left(P_t^{y'} - P_t^{y''}\right), \tag{23}$$

where P_t^y represents the power control matrix after mutation, Γ_{t-1} means the current number of iterations, and $t > 1$; $P_t^{y'}$ and $P_t^{y''}$ represent any two power control matrices in the current iteration, and $y' \ne y''$.

Γ_{t-1} means the success rate of the $(t-1)$th iteration and is defined as

$$\Gamma_{t-1} = \sum_{y=1}^{Y}\frac{1}{Y}V_{t-1}^y, \tag{24}$$

where Y means the salp number and V_{t-1}^y represents the success value.

If the fitness value of the yth salp in the tth iteration is greater than that in the $(t-1)$th iteration, the tth iteration of the yth salp is considered to succeed. Thus, the success value is defined as

$$V_{t-1}^{y} = \begin{cases} 0, & F(A^{y}, P^{y}) < F\left(A^{y-1}, P^{y-1}\right), \\ 1, & F(A^{y}, P^{y}) \geq F\left(A^{y-1}, P^{y-1}\right). \end{cases} \tag{25}$$

(2) *Leader-Follower Adaptive Adjustment Strategy*. The calculation formula of the proposed leader-follower number is

$$\begin{aligned} &\text{leader salps} : \rho N, \\ &\text{follower salps} : (1-\rho)N, \end{aligned} \tag{26}$$

where ρ means the weight and is calculated by

$$\rho = \left| \mu \times \left[\sin\left(-\frac{\pi t}{2T} + \frac{\pi}{2} \right) - \widehat{f} \times \theta \right] \right|, \tag{27}$$

where μ is the scale factor of leader-follower and t and T represent the current iteration and maximum iteration, respectively. $\widehat{f}$ is the perturbation deviation factor, and θ is an interval of $[0, 1]$.

The leader salp positions are updated by

$$\begin{aligned} A^{y\wedge} &= A^{y\wedge}, \\ P^{y\wedge} &= \begin{cases} P_{\text{best}} + \lambda_1 \lambda_2 P_d^{\max}, & \lambda_3 \geq 0.5, \\ P_{\text{best}} - \lambda_1 \lambda_2 P_d^{\max}, & \lambda_3 < 0.5, \end{cases} \end{aligned} \tag{28}$$

where $1 \leq \widehat{y} \leq \rho N$, $A^{y\wedge}$ and $P^{y\wedge}$ are leader salp positions. P_{best} is defined as the current optimal power control matrix in the iterative process. $\lambda_1 = 2e^{-(4t/T)^2}$, λ_2 and λ_3 are intervals of $[0, 1]$, respectively. $P_d^{\max}$ represents the maximum power constraint.

The follower salps' positions are defined as

$$\begin{aligned} A^{y} &= \begin{cases} A^{y}, & F(A^{y}, P^{y}) \geq F\left(A^{y'''}, P^{y'''}\right), \\ A^{y'''}, & F(A^{y}, P^{y}) < F\left(A^{y'''}, P^{y'''}\right), \end{cases} \\ P^{y} &= \begin{cases} P^{y} + \left(\mu_1 - \dfrac{\mu_2 t}{T}\right)\left(P^{y} - P^{y'''}\right), & F(A^{y}, P^{y}) \geq F\left(A^{y'''}, P^{y'''}\right), \\ P^{y} - \left(\mu_1 - \dfrac{\mu_2 t}{T}\right)\left(P^{y} - P^{y'''}\right), & F(A^{y}, P^{y}) < F\left(A^{y'''}, P^{y'''}\right), \end{cases} \end{aligned} \tag{29}$$

Table 1: Default parameters.

Parameter	Value
Cell coverage (m^3)	$1000 * 1000 * 100$
Number of UEs	200
Noise spectral density (dBm/Hz)	−174
Target SINR value (γ_0) (dB)	10
Shadowing standard deviation (dB)	8
Path loss exponent (α)	4
Circuit power of the devices (mW)	50
Transmit power of CUEs (dBm)	23
Maximum transmit power of D2D (dBm)	23
SE threshold of D2D pairs	0~12
D2D pair distance (m)	10~30
Number of UAVs	5~9
q	9.6
φ	0.16
η_{Los}	1
η_{NLos}	20

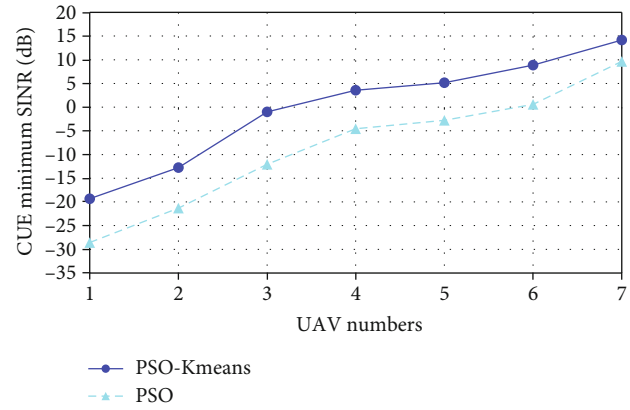

Figure 4: Convergence of PSO and PSO-Kmeans for UAV number versus CUE minimum SINR.

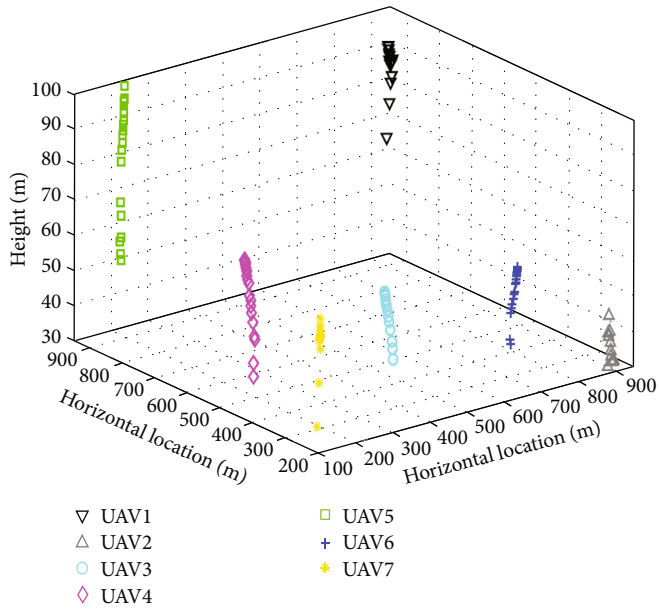

Figure 5: UAV 3D locations.

where $\rho N \le y \le N$, A^y and P^y are follower salp positions. $A^{y'''}$ and $P^{y'''}$ is salp position that salp y chooses to follow according to the Q-learning strategy. μ_1 and μ_2 are weight value, which $\mu_1 = 0.8$ and $\mu_2 = 0.6$. $F(A^y, P^y)$ is represented for the fitness function that $F(A^y, P^y) = \mathrm{EE}(A^y, P^y)$.

(3) *Q -Learning Strategy*. Q-learning strategy includes state, action, reward, and value. The current position of the salp y (whether it is a follower salp or a leader salp) is the state $\hat{s}_y$, and the current positions of all salps constitute the state space $\hat{S}$. The movement of the salp y following another salp y''' is an action $\hat{a}_y$, and all the actions of the salp swarm constitute the action space $\hat{A}$. The maximum value is the strategy of salp action selection. Following the action, the state of each salp transitions to a new state receives a reward $r\wedge^{(y,y''')}$.

(i) *Agent*. Salp $\forall y \in \mathcal{Y} = \{1, 2, \cdots, Y\}$.

(ii) *State*. The current position of the salp y.

(iii) *Action*. The movement of the salp y follows another salp y'''. 1 means the salp y can follow the salp y'''; 0 denotes the salp y cannot. Meanwhile, a leader salp is only allowed to choose another leader with the highest value to follow.

(iv) *Reward*. The reward function is formulated by the fitness function $F(A^y, P^y) = \mathrm{EE}(A^y, P^y)$. If the action that the salp y carries out can improve the current maximum fitness value of the salp swarm, the action gets a 20-point reward. If the action that the salp y carries out can improve the fitness value $F(A^y, P^y)$ compared with the last iteration, the action gets a 5-point reward; the agent receives a −5-point reward if otherwise. Thus, the reward function can be expressed as

$$r\wedge^{(y,y''')} = \begin{cases} 20, & \text{if } F_t^y > F_{t-1}^{\text{best}}, \\ 5, & \text{if } F_t^y > F_{t-1}^y, \\ -5, & \text{if } F_t^y < F_{t-1}^{\text{y}}. \end{cases} \tag{30}$$

(v) *Value*. The value function is defined as long-term return, which can be regarded as a cumulative reward. The value function can be expressed as

$$Q^{(y,y''')} = r\wedge^{(y,y''')} + \epsilon \max Q^{(y)}, \tag{31}$$

where ϵ means the discount factor.

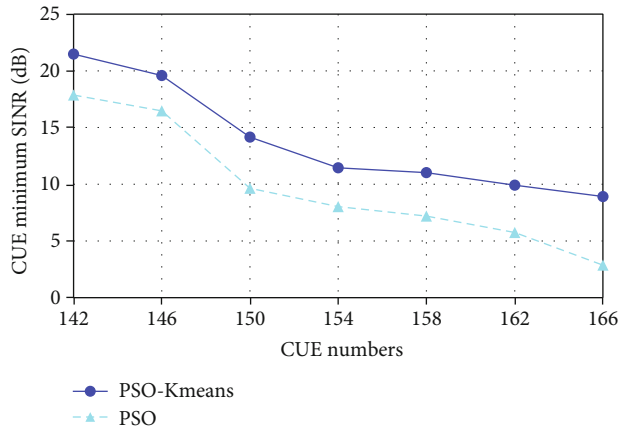

Figure 6: CUE minimum SINR versus CUE number.

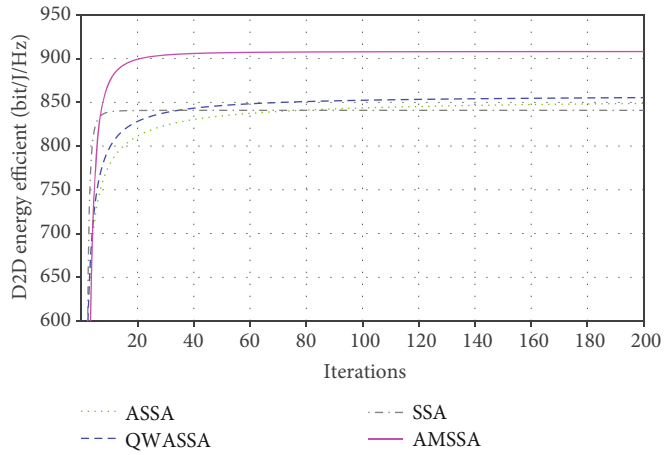

Figure 7: Convergence of four algorithms for iterations versus D2D EE.

The AMSSA algorithm is shown in Algorithm 2.

6. Simulation Results

In this section, simulation results verify the theoretical analysis and the effectiveness of the proposed approaches. In the simulations, a community of 1000 square meters without GBSs is considered. Therefore, UAV-BSs are used to provide communication for users in the cell. In addition, assumed that in a short time, the UAV-BSs are in a static state and can provide communication for users within the signal coverage range stably. D2D pairs are generated by the distance between two CUEs (i.e., if the distance between two CUEs is less than a constant value, the two CUEs are carried out D2D communication). Firstly, we use the PSO-Kmeans clustering algorithm to minimize the UAV number in our system and deploy the UAVs' positions. Moreover, the air to ground models described in [11] are used to model the path loss with $q = 9.6$, $\varphi = 0.16$, $\eta_{\text{Los}} = 1$, and $\eta_{\text{NLos}} = 20$. Secondly, AMSSA is used to solve the D2D energy efficiency maximization scheme in the D2D-abled UAV-based system. Default parameters in the simulations are given in Table 1.

Figure 4 shows the change of the minimum SINR of CUEs in the system with the increasing number of UAVs. As can be seen from Figure 4, to reach the SINR threshold $\gamma_0 = 10$ dB, 7 UAVs need to be deployed by the PSO-Kmeans algorithm, but more UAVs need to be deployed through the PSO algorithm. Under the same distribution of CUEs and the same number of UAVs, the PSO-Kmeans algorithm can find better UAV deployment than that of the PSO algorithm, which makes CUEs get better communication quality. Compared with the random initialization, Kmeans clustering initialization can get a better initial point, which leads to the deployment of fewer UAVs to achieve higher SINR. With the increase of deployed UAVs in the system, the minimum SINR of CUEs increases. When the total number of CUEs is constant but the number of UAVs increases, the number of CUEs covered by each UAV decreases, and each cellular user can allocate more transmission power. The rate of transmission power increase is greater than that of interference increase, so the minimum SINR increases and the communication quality of CUEs improves.

Figure 5 shows the 3D position update process of seven UAVs with the SINR threshold $\gamma_0 = 10$ dB. We can find that the UAVs' positions converge quickly only after a few generations.

Figure 6 shows the performance of the PSO-Kmeans algorithm and PSO algorithm under the condition of a constant number of UAVs. The minimum SINR of CUEs decreases with the increase of the total number of CUEs. The more the number of CUEs in the system and the more the number of CUEs covered by each UAV, the smaller the transmission power allocated to each CUE, and the smaller the minimum SINR in the system. In other words, to achieve the required SINR threshold, the more cellular users, the more UAVs are needed. It can be seen from Figure 6 that when the number of CUEs is equal to 150 and the number of UAVs is equal to 7, the UAV deployment optimized by the PSO-Kmeans algorithm can meet the minimum threshold of SINR, but the PSO algorithm cannot meet.

Figure 7 shows the fitness convergence curves of the SSA, the ASSA, the QWASSA, and our proposed AMSSA. The minimum rate is set to 2 bit/s/Hz. Compared with the other three algorithms, AMSSA can significantly improve the efficiency of D2D pairs. AMSSA can quickly converge to a better value in a shorter time. Therefore, AMSSA is not easy to fall into local optimum, and its search accuracy is higher. This is because the AMSSA adopts population variation strategy and adaptive follower position updating and leader-follower number updating, which has strong local mining ability and global searching ability.

Figure 8 compares the performance of D2D pairs EE of the SSA, the ASSA, the QWASSA, and our proposed AMSSA for different D2D pair distances, but the deployment of UAVs in the system keeps the same. The minimum rate is set to 2 bit/s/Hz. With the increase of the distance between D2D_R and D2D_T, the EE of D2D pairs in the system increases monotonically due to the increase of the number of D2D pairs. However, compared with the other three

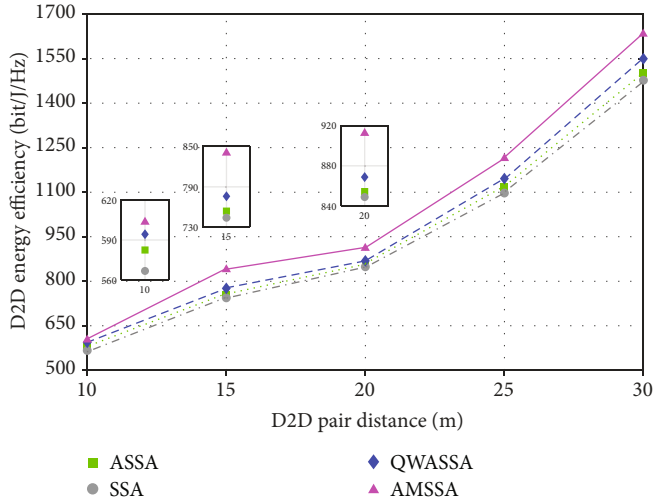

Figure 8: D2D pair distance versus D2D EE.

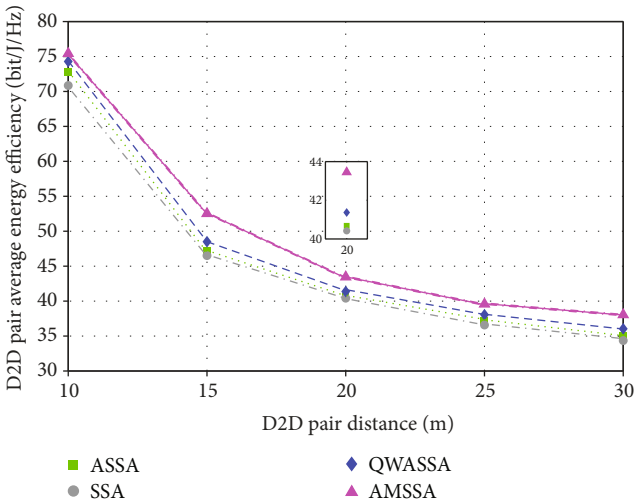

Figure 9: D2D pair distance versus D2D pair average energy efficiency.

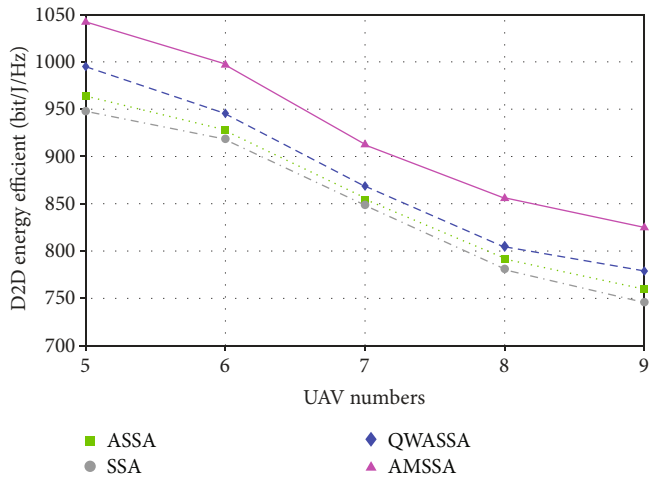

Figure 10: UAV numbers versus D2D EE.

algorithms, the AMSSA can make the system more energy-efficient for different distances.

Figure 9 shows the average EE at different distances for the same UAV deployment. Although the total D2D EE increases, which is shown in Figure 9, the average EE decreases. The minimum rate is set to 2 bit/s/Hz. The more D2D pairs that each UAV-BS controlled, the greater intercell and intracell interference between D2D pairs, and the lower average EE. However, compared with the SSA, the ASSA, and the QWASSA, the D2D EE of the proposed AMSSA decreases slower.

Figure 10 shows the relationship between D2D EE and the numbers of UAV in the system, and the distribution of D2D pairs keeps the same. The minimum rate is set to 2 bit/s/Hz. As the number of UAVs increases, the D2D EE decreases monotonously. It means that when the numbers of D2D pairs are fixed and the numbers of UAVs increase, the D2D pairs will produce more intercell interference, resulting in a decrease of D2D EE in the system. Although the system D2D EE of the AMSSA scheme decreases with the increase of the UAV number, its performance remains superior to the other three baseline algorithms.

7. Conclusion

In this paper, we investigate the UAV deployment, the channel allocation, and power control problem of D2D pairs in the D2D-abled UAV-based system. Firstly, we minimize UAVs' number and deployment to satisfy a given SINR requirement by using the PSO-Kmeans algorithm. After determining the UAV deployment in the system, we aim to maximize the energy efficiency of D2D pairs while guarantying the QoS of networks. The problem of D2D pairs' channel allocation and power control is a complicated NP-hard problem. To solve this problem, we propose the AMSSA algorithm. The population variation strategy mutates the nonoptimal individuals, which can increase the possibility that they become the optimal individuals in the

next iteration and improve the ability of the algorithm to jump out of the local optimal. The adaptation of leader-follower numbers leads to faster convergence speed and more excellent local mining capability of the AMSSA. Meanwhile, the position update mode of leader salps makes iterations more difficult to fall into local optimization. The AMSSA performs the best in terms of D2D pair energy efficiency in the D2D-abled UAV-based system compared with the other benchmark schemes.

Data Availability

The data used to support the findings of this study are included within the article.

Conflicts of Interest

The authors declare that they have no conflicts of interest.

Acknowledgments

This work is supported by the China Postdoctoral Science Foundation under Grant No. 2018M640032, the Beijing Postdoctoral Science Foundation under Grant No. ZZ2019-73, the National Natural Science Foundation of China under Grant Nos. 61571021, 61701010, and U1633115, and the Seed Fund for International Scientific Research Cooperation under Grant No. 2021-A02.

References

[1] K. M. S. Huq, S. Mumtaz, J. Rodriguez, P. Marques, B. Okyere, and V. Frascolla, "Enhanced C-RAN using D2D network," *IEEE Communications Magazine*, vol. 55, no. 3, pp. 100–107, 2017.

[2] Y. Zeng, R. Zhang, and T. J. Lim, "Wireless communications with unmanned aerial vehicles: opportunities and challenges," *IEEE Communications Magazine*, vol. 54, no. 5, pp. 36–42, 2016.

[3] K. Wang, R. Zhang, L. Wu et al., "Path loss measurement and modeling for low-altitude UAV access channels," in *2017 IEEE 86th Vehicular Technology Conference (VTC-Fall)*, pp. 1–5, Toronto, ON, Canada, September 2017.

[4] B. Li, C. Chen, R. Zhang, H. Jiang, and X. Guo, "The energy-efficient UAV-based BS coverage in air-to-ground communications," *2018 IEEE 10th Sensor Array and Multichannel Signal Processing Workshop (SAM)*, 2018, pp. 578–581, Sheffield, July 2018.

[5] N. Zhao, W. Lu, M. Sheng et al., "UAV-assisted emergency networks in disasters," *IEEE Wireless Communications*, vol. 26, no. 1, pp. 45–51, 2019.

[6] W. J. Shi, Y. J. Sun, M. Liu et al., "Joint UL/DL resource allocation for UAV-aided full-duplex NOMA communications," *IEEE Transactions on Communications*, p. 1, 2021.

[7] B. Li, S. Zhao, R. Zhang, and L. Yang, "Full-duplex UAV relaying for multiple user pairs," *IEEE Internet of Things Journal*, vol. 8, no. 6, pp. 4657–4667, 2021.

[8] P. Qin, Y. Zhu, X. Zhao, X. Feng, J. Liu, and Z. Zhou, "Joint 3D-location planning and resource allocation for XAPS-enabled C-NOMA in 6G heterogeneous Internet of Things," *IEEE Transactions on Vehicular Technology*, vol. 70, no. 10, pp. 10594–10609, 2021.

[9] H. Qu, W. Zhang, J. Zhao, Z. Luan, and C. Chang, "Rapid deployment of UAVs based on bandwidth resources in emergency scenarios," in *2020 Information Communication Technologies Conference (ICTC)*, pp. 86–90, Nanjing, China, March 2020.

[10] Z. Yuheng, Z. Liyan, and L. Chunpeng, "3-D deployment optimization of UAVs based on particle swarm algorithm," in *2019 IEEE 19th International Conference on Communication Technology (ICCT)*, pp. 954–957, Xi,an, China, October 2019.

[11] W. Liu, G. Niu, Q. Cao, M.-O. Pun, and J. Chen, "Particle swarm optimization for interference-limited unmanned aerial vehicle-assisted networks," *IEEE Access*, vol. 8, pp. 174342–174352, 2020.

[12] H. Yang, R. Ruby, Q.-V. Pham, and K. Wu, "Aiding a disaster spot via multi-UAV-based IoT networks: energy and mission completion time-aware trajectory optimization," *IEEE Internet of Things Journal*, 2021.

[13] X. Liu, Y. Liu, and Y. Chen, "Reinforcement learning in multiple-UAV networks: deployment and movement design," *IEEE Transactions on Vehicular Technology*, vol. 68, no. 8, pp. 8036–8049, 2019.

[14] J. Liu, Q. Wang, X. Li, and W. Zhang, "A fast deployment strategy for UAV enabled network based on deep learning," in *2020 IEEE 31st Annual International Symposium on Personal, Indoor and Mobile Radio Communications*, pp. 1–6, London, UK, August 2020.

[15] A. H. Arani, M. Mahdi Azari, W. Melek, and S. Safavi-Naeini, "Learning in the sky: towards efficient 3D placement of UAVs," in *2020 IEEE 31st Annual International Symposium on Personal, Indoor and Mobile Radio Communications*, pp. 1–7, London, UK, August 2020.

[16] Z. Wang and L. Duan, "Chase or wait: dynamic UAV deployment to learn and catch time-varying user activities," *IEEE Transactions on Mobile Computing*, p. 1, 2021.

[17] L. Ruan, J. Wang, J. Chen et al., "Energy-efficient multi-UAV coverage deployment in UAV networks: a game-theoretic framework," *China Communications*, vol. 15, no. 10, pp. 194–209, 2018.

[18] S. Ahmed, M. Z. Chowdhury, and Y. M. Jang, "Energy-efficient UAV-to-user scheduling to maximize throughput in wireless networks," *IEEE Access*, vol. 8, pp. 21215–21225, 2020.

[19] C. Zhan and G. Yao, "Energy efficient estimation in wireless sensor network with unmanned aerial vehicle," *IEEE Access*, vol. 7, pp. 63519–63530, 2019.

[20] S. Yin and F. R. Yu, "Resource allocation and trajectory design in UAV-aided cellular networks based on multi-agent reinforcement learning," *IEEE Internet of Things Journal*, 2021.

[21] J. Ji, K. Zhu, D. Niyato, and R. Wang, "Joint trajectory design and resource allocation for secure transmission in cache-enabled UAV-relaying networks with D2D communications," *IEEE Internet of Things Journal*, vol. 8, no. 3, pp. 1557–1571, 2021.

[22] K. M. S. Huq, S. Mumtaz, Z. Zhou, K. Chandra, I. E. Otung, and J. Rodriguez, "Energy-efficiency maximization for D2D-enabled UAV-aided 5G networks," in *ICC 2020-2020 IEEE International Conference on Communications (ICC)*, pp. 1–6, Dublin, Ireland, June 2020.

[23] B. Wang, J. Ouyang, W. Zhu, and M. Lin, "Optimal altitude of UAV-BS for minimum boundary outage probability with

imperfect channel state information," in *2019 IEEE/CIC International Conference on Communications in China (ICCC)*, pp. 607–611, Changchun, China, August 2019.

[24] K. Doppler, M. P. Rinne, P. Janis, C. B. Ribeiro, and K. Hugl, "Device-to-device communications," in *Functional Prospects for LTE-Advanced Networks, IEEE ICC*, pp. 1–6, Shanghai, June 2009.

[25] Z. Zhou, M. Dong, K. Ota, G. Wang, and L. T. Yang, "Energy-efficient resource allocation for D2D communications underlaying cloud-RAN based LTE-A networks," *IEEE Internet of Things Journal*, vol. 3, no. 3, pp. 428–438, 2016.

[26] A. Al-Hourani, S. Kandeepan, and S. Lardner, "Optimal LAP altitude for maximum coverage," *IEEE Wireless Communications Letters*, vol. 3, no. 6, pp. 569–572, 2014.

[27] S. Mirjalili, A. H. Gandomi, S. Z. Mirjalili, S. Saremi, H. Faris, and S. M. Mirjalili, "Salp swarm algorithm: a bio-inspired optimizer for engineering design problems," *Advances in Engineering Software*, vol. 114, no. 6, pp. 163–191, 2017.

[28] Z. Huang, Y. L. Yang, D. Y. Yang, and K. Mao, "Study on energy efficiency of D2D communication system based on improved salp group algorithm," *High Technology Letters*, vol. 30, no. 8, pp. 790–797, 2020.